NUMERICAL INVESTIGATION ON THE EFFECTS OF VORTEX SHEDDING ON BOUNDARY LAYER UNSTEADINESS

A.B.M. Toufique Hasan* and Dipak Kanti Das
Department of Mechanical Engineering,
Bangladesh University of Engineering and Technology (BUET),
Dhaka-1000, Bangladesh.
*Corresponding address: toufiquehasan@me.buet.ac.bd

Abstract: *The interaction between an initially laminar boundary layer developed spatially on a flat plate under the influence of vortex shedding induced from a rotating circular cylinder has been simulated numerically. The rotational speed of the cylinder is varied to generate the vortex shedding of different intensities. Also the flat plate is kept at different positions from the cylinder. Due to asymmetry in the flow field, the present problem is governed by unsteady Navier-Stokes equations which are simulated numerically by finite element method. Computations are carried out for low Reynolds number range up to 1000. Instantaneous development of the flow field, unsteady boundary layer integral parameters, and wall skin friction are presented on different streamwise locations over the plate. From the computation, it is observed that the vortex shedding substantially affects the boundary layer development. The disturbed displacement and momentum thicknesses of the plate increase up to 1.6 times and 2.6 times of the undisturbed flow, respectively. Also the plate shape factor approaches a value of 1.5 which is typical for turbulent flow. This interaction strongly depends on the rotating speed of the cylinder, the relative positions of the cylinder and the plate and also on Reynolds number of the flow.*

Keywords: *Vortex shedding, finite element, boundary layer, wall skin friction.*

INTRODUCTION

In multistage turbomachines, owing to the alternating arrangement of the rows of stationary and rotating blades, the boundary layer developing on a blade is periodically subjected to the wakes of upstream blades. The wake exhibits a defect in mean velocity and a superimposed high level of turbulence intensity. These conditions have a significant influence upon the boundary layer transition process; a good understanding of which is very important for the improvement of the design of turbomachines. The boundary layer state greatly influences skin friction, drag loss, and boundary layer separation. Since in turbulent region, the heat transfer coefficients are much higher, the location of the onset of transition is of importance for the sizing and shaping of blade cooling in gas turbine engines. In recent years, gas turbine aerodynamicists have focused their attention on improving the efficiency and performance of the low pressure turbine (LPT) components. The periodic unsteady nature of the incoming flow associated with wakes substantially influences the boundary layer development including the onset and the extent of laminar separation and its turbulent re-attachment.

Goldstein and Leib[1] considered the effect of a small-amplitude, steady, streamwise vorticity field on the flow over an infinitely thin flat plate in an otherwise uniform stream. They showed how the initial linear perturbation, ultimately leads to a small-amplitude but non-linear cross-flow far downstream the leading edge. This motion was imposed on the boundary-layer flow and eventually caused the boundary layer to separate. Yang and Abdalla[2] employed LES (Large Eddy Simulation) to investigate a separated boundary layer transition under 2% free-stream turbulence on a flat plate with a blunt leading edge. The Reynolds number based on the inlet free stream velocity and the plate thickness was 6500. They observed that the effect of free-stream turbulence had led to an early breakdown of the boundary layer, and hence increased the randomization in the vertical structures.

Nomenclature

a	radius of the cylinder
c_f	wall skin friction Co-efficient
d	diameter of the cylinder
H	shape factor (δ_1/θ)
u, v	velocity components
P	pressure
X,Y	cartesian co-ordinates
x	axial distance from plate leading edge
y	vertical distance from plate leading edge
Re_d	Reynolds number, U_{free} d/ ν
t	time
Greeks	
α	speed ratio, $\omega a/U_{free}$
δ_1	displacement thickness
θ	momentum thickness
μ	dynamic viscosity of the fluid
ν	kinematic viscosity of the fluid
ρ	density of the fluid
τ	global dimensionless time, ut/d
ω	rotational speed of the cylinder
Subscripts	
av	average value
c	cylinder position
p	streamwise location over the plate
Superscripts	
*	local value

The nonlinear effects of longitudinal vorticity elements in boundary layers were studied by Sabry and Liu[3] to elucidate the nonlinearity producing sites of secondary instability and turbulent generator. They found mushroom-like velocity contours surrounding the peak as well as the streamwise velocity profiles in the peak and valley regions, which agreed well with experimental measurements up to the region of expected secondary instabilities.

The accelerated decay of aircraft wake vortices in a convectively driven and evolving atmospheric boundary layer was investigated by means of LES by Holzäpfel et al.[4]. It was shown that the wake vortices were rapidly deformed at scales of the alternating updraft and downdraft regions and the segments of the wake vortices could stall at flight level but they were quickly eroded by the turbulent updrafts at the same time. Lee and Gerontakos[5] studied the characteristics of the unsteady boundary layer and stall events occurring on an oscillating NACA 0012 airfoil by using closely spaced multiple hot-film sensor arrays at $Re=1.35x10^5$. The existence of disturbed laminar, transitional and turbulent flow on a turbine blade had been demonstrated by Addison and Hodson[6,7]**.** They found that the start of transition was unsteady and dominated by stator wake turbulence. The transition process was characterized by the appearance of high frequency bursts above the lower frequency background disturbances. They also investigated the significance of the wake jet and unsteady frequency parameter. Supporting experiments were carried out in a linear cascade with varying inlet turbulence, together with a simple unsteady transition model explaining the featured seen in the turbine. A detailed experimental study on the behavior of the separated zone on the suction surface of a highly loaded LPT-blade under periodic unsteady wake flow was presented by Schobeiri et al.[8]**.** Two-dimensional periodic unsteady inlet flow was simulated by the translational motion of a wake generator, with a series of cylindrical rods attached to two operating timing belt driven by an electric motor. One steady and two different unsteady inlet wake flow conditions with corresponding wake frequencies and velocities and turbulence intensities were investigated at Re=50000, 75000, 100000 and 125000 based on blade suction surface length. They found the periodic behavior of the boundary layer integral parameters. Numerical simulation on the interaction of axial compressor stator with upstream rotor wakes and tip leakage vortices were employed to elucidate their impact on the time-averaged performance of the stator by Volkov and Tau[9]. They concluded that the impact of stator interaction with upstream wakes and vortices depended on the parameters such as axial spacing, loading, and the frequency of wake fluctuations in the rotor frame. At a reduced spacing, this impact became significant. The most import aspect of the tip vortex was the relative velocity defect and the associated relative total pressure defect.

Wu et al.[10] numerically simulated the interaction between an initially laminar boundary layer developing spatially on a flat plate and wakes. The flow resembles to the transitional boundary layer on turbomachinery blades. They found that the inlet wake disturbances inside the boundary layer evolved rapidly into longitudinal puffs during an initial receptivity phase. In the absence of strong forcing from free-stream vortices, these structures exhibited streamwise elongation with gradual decay in amplitude. Turbulent wakes swept across a flat plate boundary layer was simulated by Wu and Durbin[11]. Benchmark data from a direct numerical simulation of this process were presented and compared to Reynold-averaged predictions. The data included averaged skin-friction and mean velocities. Investigations of boundary layer transition in undistributed flow and in flow periodically disturbed by wakes were carried out based on extensive hot-wire measurements by Orth[12]. The measurements were carried out in a low speed wind tunnel with a rotating cascade upstream of the testing section, where a flat plate of 700 mm length and 20 mm thickness (d) was mounted at half height. The rotating cascade consists of two disks. Three bars of 2 mm diameter were fixed between the disks. The bar moved on a circular path perpendicular to the flow in front of the plate, so that the wakes hit the plate periodically. This setup is chosen to simulate conditions in turbomachines, where the blades are often subjected to periodic wakes of upstream blade rows. The boundary layer in a flow periodically disturbed by wakes differs in two ways from a boundary layer developing in an undisturbed flow. First, an early onset of transition is observed momentarily as the high turbulence level of the wake disturbs the boundary layer and leads to the formation of a turbulent patch. Second, laminar becalmed regions are formed behind the turbulent patches. The results also show that with increasing turbulence intensity, the onset of transition shifts to lower Reynolds number, and the effect of pressure gradient almost disappears. Liu and Rodi[13] investigated in detail by hot-wire measurements the boundary layer developing along a flat plate over which wakes passed periodically. The wakes were generated by cylinders moving on a squirrel cage in front of the plate leading edge. The Reynolds number was fairly low so that the boundary layer remained laminar over the full length when no disturbing wakes were present. The influence of wake passing frequency on the boundary-layer development and in particular on the transition processes was examined. When wakes passed over the plate, the boundary layer was found to be turbulent quite early underneath the free-stream disturbances due to wakes, while it remained initially laminar. The turbulent boundary layer stripes underneath the disturbed free-stream traveled downstream and grew together so that the embedded laminar regions disappear and the boundary layer became fully turbulent. The streamwise locations where this happen moved upstream with increasing wake-passing frequency, and a correlation was established in this experiment. A study had been made of the process of laminar to turbulent transition induced by a von Karman vortex street, in the boundary layer on a flat plate by Kyriakides et al.[14]**.** Hot-wire measurements over a range of Strouhal frequencies and free stream velocities were used for the identification of the transition onset. It was established that, the onset of the strong Von Karman wake induced transition process was a function of the free stream velocity, the position of the cylinder with respect to the plate, the cylinder diameter, the drag coefficient and the minimum velocity in the developing wake.

Although there are a number of experimental investigations on the flow around flat plate under the influence of cylinder wake placed at various heights, numerical investigations is limited due to its complexity in grid generation. Also wake induced from a rotating circular cylinder got less attention in this regard. In the present work, a numerical study of this type of flow on laminar Reynolds number ranges is considered and the influence of vortex shedding on plate boundary layer unsteadiness specially on instantaneous development of the flow field, boundary layer and the wall skin friction are investigated.

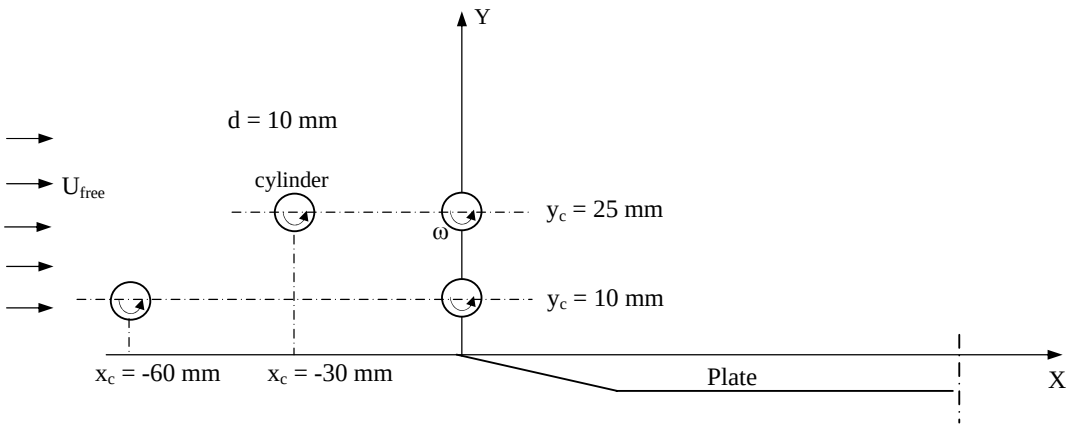

Figure 1. Cylinder positions for all test cases.

MATHEMATICAL MODELING

Figure 1 shows the schematic diagram of the physical model of the present study where a circular cylinder of 10mm diameter is rotating at constant angular velocity ω in counterclockwise direction in front of a flat plate of 10mm thickness and 0.6m length in an otherwise uniform free stream with velocity U_{free}.

The governing equations for two-dimensional, unsteady, viscous, incompressible flow with negligible body force can be written in the following form:

Continuity equation:

$$\frac{\partial u}{\partial x} + \frac{\partial v}{\partial y} = 0 \qquad (1)$$

X-momentum equation:

$$\rho\left(\frac{\partial u}{\partial t} + u\frac{\partial u}{\partial x} + v\frac{\partial u}{\partial y}\right) = -\frac{\partial P}{\partial x} + \mu\left(\frac{\partial^2 u}{\partial x^2} + \frac{\partial^2 u}{\partial y^2}\right) \qquad (2)$$

Y-momentum equation:

$$\rho\left(\frac{\partial v}{\partial t} + u\frac{\partial v}{\partial x} + v\frac{\partial v}{\partial y}\right) = -\frac{\partial P}{\partial y} + \mu\left(\frac{\partial^2 v}{\partial x^2} + \frac{\partial^2 v}{\partial y^2}\right) \qquad (3)$$

The computational domain subjected to initial condition,

$$(u, v)\,|_{t=0} = (U_{free}, 0) \qquad (4)$$

The boundary conditions considered for the present problem are as follows:

1. An inflow boundary condition is applied at the left boundary:

$$u = U_{free} \text{ and } v = 0 \qquad (5)$$

2. An outflow boundary condition at the right boundary:

$$\frac{\partial u}{\partial x} = 0 \quad \text{and} \quad \frac{\partial v}{\partial x} = 0 \qquad (6)$$

3. No-slip velocity condition is employed for all velocity components on all solid walls. Thus,

- On the plate surface, u = v =0. (7)
- On the surface of the cylinder the velocity is equal to the angular velocity, ω. Then, $u = \omega_X$ and $v = \omega_Y$ (8)

SOLUTION METHODOLGY

The numerical solution of the governing partial differential equations for the present study is based on finite element method (FEM). Mixed finite element formulation for velocity and pressure is used. The computational domain is first subdivided into finite number of triangular elements. Unstructured finite element mesh is used for the discretization. Shape functions used are quadratic and linear for velocity field and pressure field, respectively. The discretized linear algebraic equations obtained from partial differential equations are solved by direct linear solver UMFPACK. The relative tolerance for error estimation of all dependent variables was 1e-6. For temporal discretization, implicit procedure is used for the present unsteady problem.

Grid sensitivity assessment:

Numerical results are greatly dependent on the grid generation in the computation domain. Due to this fact a grid refinement test with several numbers of elements is carried out to determine the optimum number of elements in the domain. A grid size of 20,000 elements was selected based on the accuracy of the results and computational time.

RESULTS AND DISCUSSION

The boundary layer development on the surface of a flat plate under the influence of vortex shedding from a rotating circular cylinder is computed numerically for different cases. The cylinder is positioned at different non-dimensional axial distance x_c/d and the non-dimensional vertical distance y_c/d from the plate leading edge. The plate has 10 mm thickness with a sharp leading edge of 0.5 mm radius. To avoid the leading edge separation the plate is placed at -0.5^0 with the undisturbed approach velocity of flow.

Instantaneous streamlines of the flow field:

Figures 2 to 4 represent the instantaneous streamline development in the flow field. From these figures, it is clear that the vortex shedding in the Von Karman vortex street creates a wall boundary layer with a strong vorticity sheet while approaching to the ground or plate. The separated vorticity sheet is elongated until it breaks and creates a secondary vortex. This vortex rolls over the plate. The breakdown of the structure is due to different propagation speeds of the leading and trailing edges of the mushroom-like structure. The leading edge is convected at $0.88U_{free}$ and the trailing edge at $0.5U_{free}$ where U_{free} is the undisturbed velocity of the approach flow[13]. In this study these velocities are not computed, but the flow field agreed well with this physical behavior. In the early stages of the

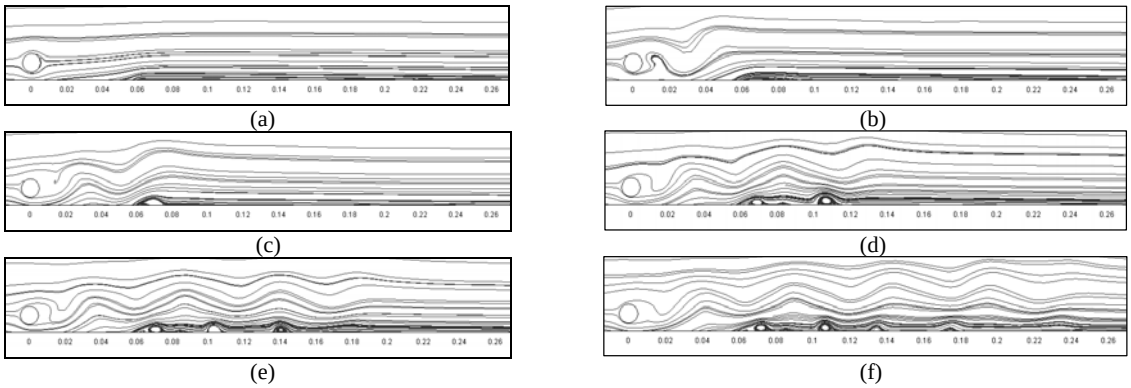

Figure 2. Instantaneous streamlines on the flow field for Re_d = 500, α = 0.5, x_c/d= -6, y_c/d=1.0; (a) τ = 1 (b) τ = 15 (c) τ = 20, (d) τ = 30, (e) τ = 40, (f) τ = 50.

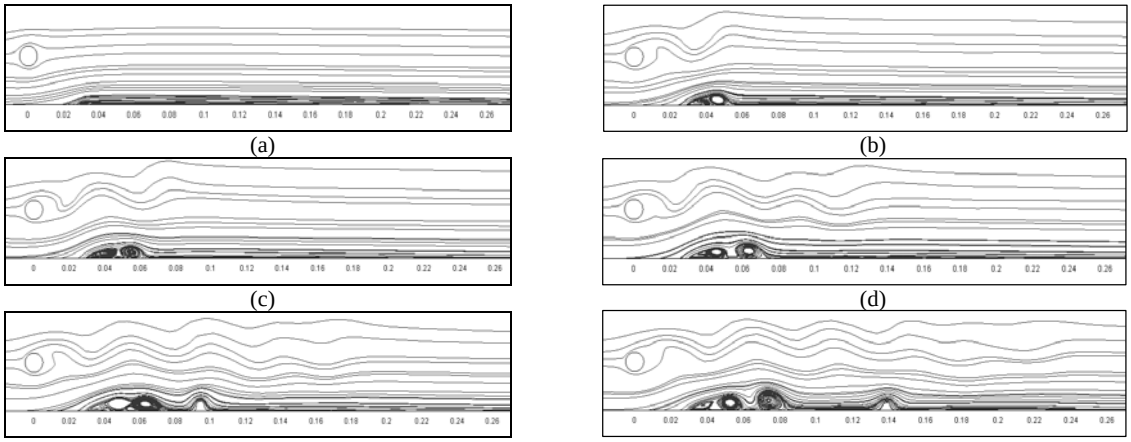

Figure 3. Instantaneous streamlines on the flow field for Re_d = 500, α = 0.5, x_c/d= -3, y_c/d=2.5; (a) τ = 1 (b) τ = 15 (c) τ = 20, (d) τ = 30, (e) τ = 40, (f) τ = 50.

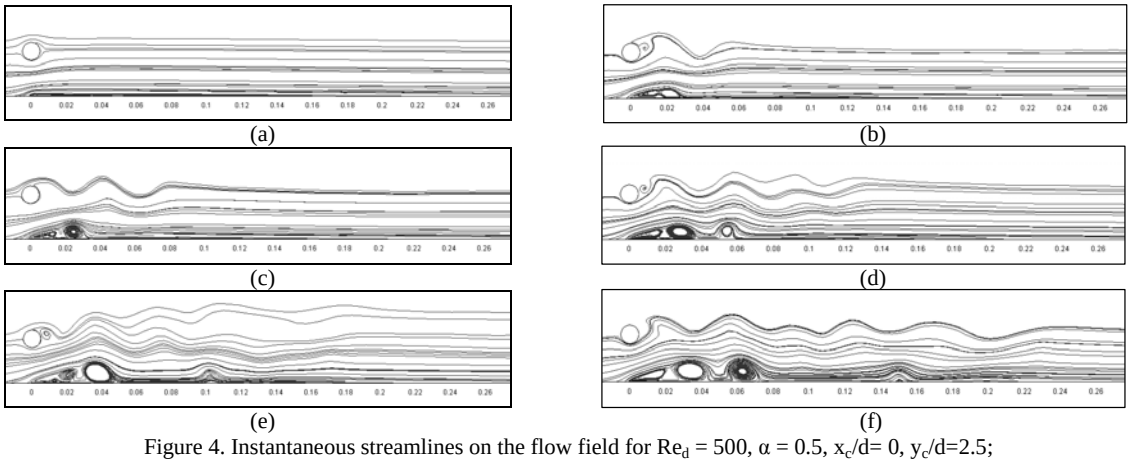

Figure 4. Instantaneous streamlines on the flow field for Re_d = 500, α = 0.5, x_c/d= 0, y_c/d=2.5; (a) τ = 1 (b) τ = 15 (c) τ = 20, (d) τ = 30, (e) τ = 40, (f) τ = 50.

development, the amplitude of the u-perturbation is small and the velocity contours show a wavy nature in the streamwise direction. The 'mushroom-like' structures for the streamwise velocity develop due to the pumping action of the counter-rotating vortices. Again the size of the 'mushroom-like' structure or core reduces in size while rolling over the plate for the higher time levels. This is due to the reduction in kinetic energy in the core i.e. due to viscous dissipation. There is always generation of 'mushroom-like' core at a very early stage from the leading edge; this core convects downstream while creating secondary instability. This secondary vortex rolls over the plate and finally disappears due to viscous dissipation.

From these figures it is observed that the time required for the core generation at the leading edge of the plate reduces while the cylinder to plate relative distance decreases. That is, when the plate approaches to the cylinder it requires less time for the formation of the core. Eventually that is due to the early interaction between the

Table 1. Time required for initial core generation for Re_d =500, α = 0.5

Cylinder to plate relative position (x_c/d y_c/d)		Time required for the initial core generation (τ)
-6	1.0	15
-3	2.5	10
0	2.5	5
0	1.0	2

Table 2. Core size for Re_d =500, α = 0.5

Cylinder to plate relative position (x_c/d y_c/d)		Core size / Cylinder diameter
-6	1.0	0.6
-3	2.5	0.75-0.9
0	2.5	1.2-1.5
0	1.0	2-3

Von Karman vortex street to the plate boundary layer. Table 1 shows the time required for initial core generation.

Again, for the same Reynolds number (Re_d) and the same speed ratio (α) the core size increases while cylinder to plate relative position decreases. Table 2 shows the relative core size for different gap ratios between cylinder and plate.

Boundary layer integral parameters:

To evaluate the quality of a designed turbomachinery blade, the displacement thickness (δ_1), momentum thickness (θ), and shape factor (H) are of particular importance. Figure 5 Shows that the boundary layer integral parameter exhibits irregular behavior with time. Interaction of vorticity elements with plate boundary layer gives rise to Reynolds stress, which affects the downstream development of the flow. This interaction always causes the thickening of the boundary layer compared to steady undisturbed flow over the plate. In case of undisturbed flow over the plate the displacement thickness (δ_1) is 1.36mm, 1.92mm, 2.72mm, and 3.33mm for x_p=50, 100, 200, 300 mm, respectively. Whereas due to the influence of vortex shedding the displacement thickness lies in the range of 1.36-1.9mm, 1.92-2.85mm, 2.72-4.05mm, and 3.33-5.1mm for x_p=50, 100, 200, 300 mm, respectively. Again for momentum thickness (θ), these values fluctuates in the range of 0.53-0.99mm, 0.74-1.6mm, 1.05-2.35mm, and 1.29-3.34mm for x_p=50, 100, 200, 300 mm, respectively, where, the first value indicates the value for undisturbed flow. For locations with higher streamwise distance, the fluctuating behavior with time is more prominent. More peak and valley regions are observed for these locations. For all the computations, the shape factor value decreases and then fluctuates monotonically from values above 2 to values below 2 whereas the shape factor value would be very close to 2.6 for the case of steady undisturbed flow over the plate. This behavior indicates that the boundary layer is always intermittently laminar

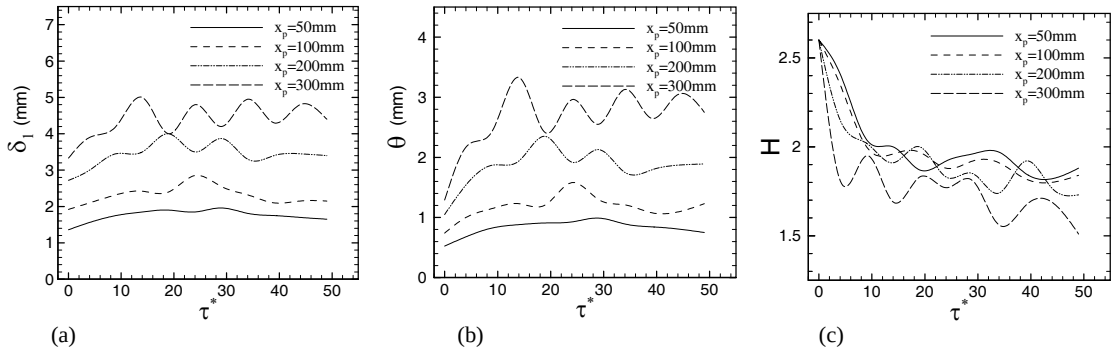

Figure 5. Temporal variation of boundary layer integral parameters for Re_d= 800, α=0.5, cylinder to plate relative position x_c/d=0, y_c/d=2.5:(a) displacement thickness (δ_1), (b)momentum thickness (θ), (c) Shape factor (H).

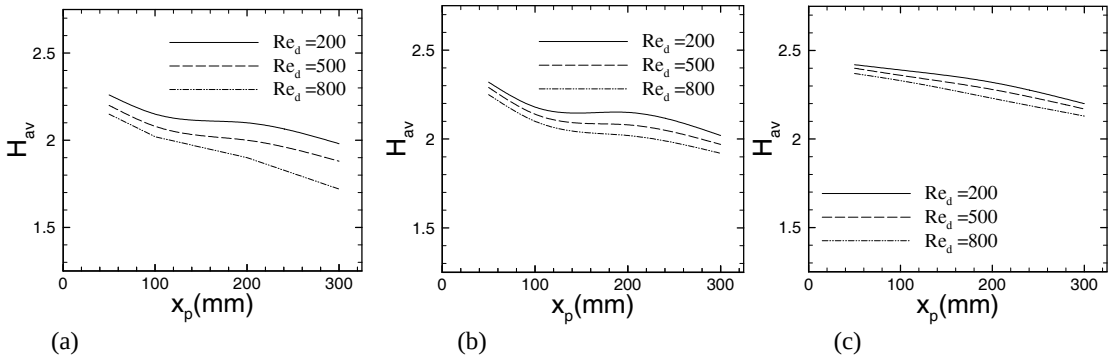

Figure 6. Average shape factor (H_{av}) variation with plate streamwise locations for different Reynolds numbers based on cylinder diameter (Re_d) for cylinder to plate relative position x_c/d= 0, y_c/d= 2.5; (a) α= 0.5, (b)α=1.0, (c) α= 1.75.

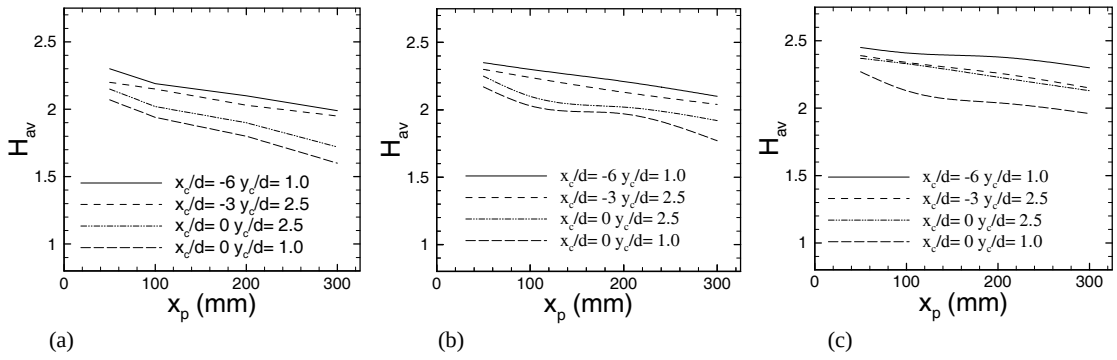

Figure 7. Average shape factor (H_{av}) variation with plate streamwise locations (x_p) for Re_d=800 and for different cylinder to plate relative positions; (a) α= 0.5, (b) α= 1.0, (c) α= 1.75.

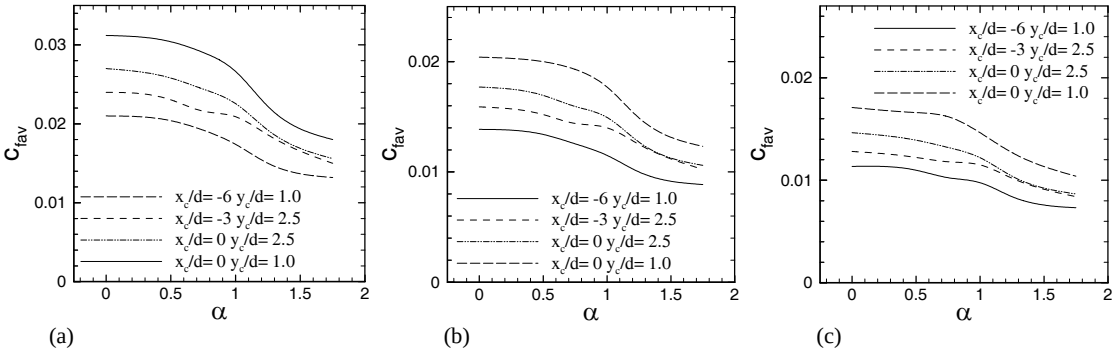

Figure 8. Variation of average skin friction co-efficient (c_{fav}) with respect to speed ratio (α) at different cylinder to plate relative position; for (a) Re_d = 200, (b) Re_d = 500, (c) Re_d = 800.

and turbulent. Also the considerable variation in boundary layer thicknesses and shape factor indicating that the transition is not fully completed and the velocity distribution over the plate is still adjusting.

Average shape factor is calculated by averaging the temporal shape factors over a time period. Figure 6 shows the average shape factor variation with plate streamwise locations for different Reynolds number at different speed ratio. From the figure it is seen that the average shape factor value decreases further downstream of the plate. Again, for all streamwise locations and also for all speed ratios, the shape factor value decreases while increasing the Reynolds number of the flow. At increased Reynolds number, the natural transition tendency can also influence the wake-boundary layer interaction phenomena. With increasing the speed ratio, the gradient of decreasing shape factor value at downstream decreases. Thus, for α = 1.75, the gradient becomes flatter compared to lower α.

Figure 7 shows the variation of average shape factor with plate streamwise locations with different cylinder-plate relative position. From these figures, it is observed that for any speed ratio, with increasing the cylinder to plate relative position, the shape factor values increases for all streamwise locations. Wake vortices looses its energy significantly before coming in contact with plate boundary layer for higher cylinder-plate relative position. For higher cylinder-plate relative position, weak wake-boundary layer interaction occurred. From Figure (a), for α = 0.5, and for x_c/d = - 6, y_c/d =1.0, the shape factor value starts nearly from 2.3 at x_p = 50 mm, whereas for x_c/d = - 3, y_c/d =2.5, the shape factor value starts nearly from 2.2 at the same location. Again for x_c/d = 0, y_c/d =2.5, the value starts from 2.15, and for x_c/d = 0, y_c/d =1.0, it starts from nearly 2.08. So, strong wake-boundary layer interaction occurs for closer cylinder-plate relative position. For other speed ratios, the profile of average shape factor distribution on different streamwise locations over the plate is comparable as described here shown in figure (b) and (c). Only the magnitude of the shape factor distribution changes for other speed ratios.

Wall Skin Friction over the plate surface:

Figure 8 shows the variation of average skin friction co-efficient with respect to speed ratio at different cylinder to plate relative positions. Figure (a) shows the variation for Re_d = 200. For Re_d = 200, the average value of skin friction co-efficient for undisturbed plate boundary layer is 0.01212 [15]. From figure, it is seen that for any cylinder to plate relative position, the disturbed skin friction by wake vortices is higher than that for undisturbed profile. Free-stream turbulence fluctuations, such as those carried by the passing wake in the present case, tend to increase skin friction. For reduction of gap between cylinder to plate, the disturbed value of skin friction is increased. This type of interaction refers to as strong-wake boundary layer interaction. For the case of x_c/d = 0, y_c/d = 1.0, the skin friction is almost 2.5 times higher than that of the undisturbed boundary layer. For far wake-boundary layer interaction, in case of x_c/d = -6, y_c/d = 1.0, the disturbed skin friction is almost 1.75 times higher than that for the case of α = 0.5. Other Reynolds number presents the same behaviour as shown in figure (b) and (c).

Figure 9 shows the average skin friction variation with respect to Reynolds number at different speed ratio.

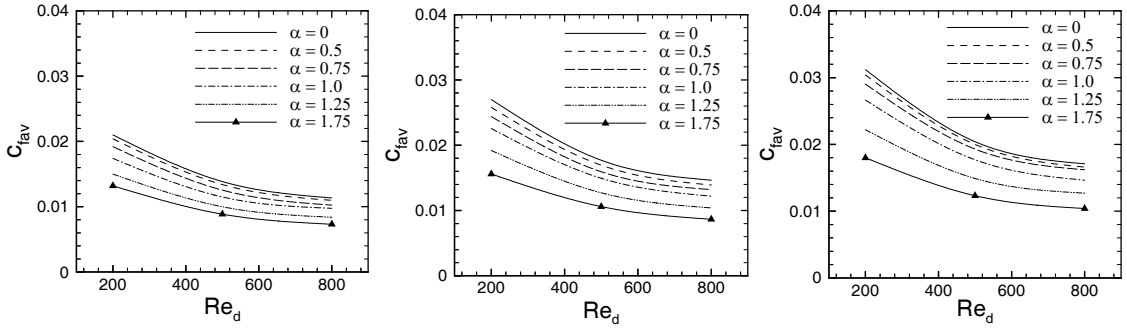

Figure 9. Variation of average skin friction co-efficient (c_{fav}) with respect to Reynolds number based on cylinder diameter (Re_d) at different speed ratio (α); (a) x_c/d= -6 y_c/d=1.0, (b) x_c/d=0 y_c/d=2.5, (c) x_c/d=0 y_c/d=1.0.

From figure (a), for any speed ratio, the average skin friction co-efficient reduces with Re_d which is found in literature. For a particular Re_d, the skin friction value reduces with increasing speed ratio. At higher speed ratio, the developed vortex shedding lies far apart from the plate surface compared to lower speed ratios. So, for higher speed ratio, the interaction of vortex with plate boundary layer becomes fragile. Thus for x_c/d = -6, y_c/d = 1.0, and for α = 1.75, the profile of skin friction value approaches very close to the undisturbed boundary layer profile. Also the other gap ratios depict the same trend.

CONCLUSIONS

Influence of vortex shedding induced from a rotating circular cylinder on the unsteady development of plate boundary layer is investigated at different ratios of peripheral speed of the cylinder to uniform velocity of the free stream. The unsteadiness is also investigated for different cylinder to plate relative positions and also for different Reynolds number. Two types of boundary layer-wake interaction are obtained from the computations; one is the strong-wake boundary layer interaction and another being the weak-wake boundary layer interaction. The strength of interaction greatly depends on the plate streamwise location, the Reynolds number of the flow, the speed ratio of the cylinder and the gap ratio between the plate and the cylinder. Strong interaction occurs when the speed ratio of the cylinder is lower. While increasing the gap ratio between the plate and the cylinder, weak interaction with boundary layer occurs due to the significant decay of the wake vortices before they come in contact with boundary layer.

REFERENCES

1. Goldstein, M. E. and Leib, S. J. 1993, "Three-dimensional Boundary-layer Instability and Separation Induced by Small-amplitude Streamwise Vorticity in the Upstream Flow", J. Fluid Mech., vol. 246, pp. 21-41.

2. Yang, Z. and Abdalla, I. E. 2005, "Effect of Free-Stream Turbulence on Large-scale Coherent Structures of Separated Boundary Layer Transition", Int. J. Numer. Meth. Fluids, vol. 49, pp. 331-348.

3. Sabry, A. S. and Liu, J. T. C. 1991, "Longitudinal Vorticity Elements in Boundary Layers: Nonlinear Development from Initial Görtler Vortices as a Prototype Problem", J. Fluid Mech., vol. 231, pp. 615-663.

4. Holzäpfel, F., Gerz, T., Frech, M. and Dörnbrack, A. 2000, "Wake Vortices in Convective Boundary Layer and Their Influence on Following Aircraft", J. Aircraft, vol. 37, No. 6, pp. 1001-1007.

5. Lee, T. and Gerontakos, P. 2004, "Investigation of Flow over an Oscillating Airfoil", J. Fluid Mech., vol. 512, pp. 313-341.

6. Addison, J. S. and Hodson, H. P. 1990, "Unsteady Transition in an Axial-Flow Turbine: Part 1-Measurements on the Turbine Rotor", J. Turbomachinery, vol. 112, pp. 206-214.

7. Addison, J. S. and Hodson, H. P. 1990, "Unsteady Transition in an Axial-Flow Turbine: Part 2 – Cascade Measurements and Modeling", J. Turbomachinery, vol. 112, pp. 215-221.

8. Schobeiri, M.T., Öztürk, B. and Ashpis, D.E., 2003, "On the Physics of Flow Along a Low Pressure Turbine Blade Under Unsteady Flow Conditions", Proc. ASME Turbo Expo Power for Land, Sea and Air, pp. 1-16.

9. Valkov, T. V. and Tan, C. S. 1999, "Effect of Upstream Rotor Vortical Disturbances on the Time-Averaged performance of Axial Compressor Stators: Part 2- Rotor Tip Vortex/Streamwise Vortex-Stator Blade Interactions", J. Turbomachinery, vol. 121, pp. 387-397.

10. Wu, X., Jacobs, R.G., Hunt, J.C.R. and Durbin, P. 1999, "Simulation of Boundary Layer Transition Induced by Periodically Passing Wakes", J. Fluid Mech., vol. 398, pp. 109-153.

11. Wu, X. and Durbin, P.A., 2000, "Boundary Layer Transition Induced by Periodic Wakes", J. Turbomachinery, vol. 122, pp. 442- 449.

12. Orth, U. 1993, "Unsteady Boundary Layer Transition in Flow Periodically Disturbed by Wakes", J. Turbomachinery, vol. 115, pp. 707-713.

13. Liu, X. and Rodi, W. 1991, "Experiments on Transitional Boundary Layers with Wake-induced Unsteadiness", J. Fluid Mech., vol. 231, pp. 229-256.

14. Kyriakides, N. K., Kastrinakis, E.G., Nychas, S.G. and Goulas, A. 1996, "Boundary Layer Transition Induced by a Von karman Vortex Street Wake", IMechE, PartG: J. Aerospace Engineering, vol. 210, pp. 167-179.

15. Schlichting, H., 1979, *Boundary Layer Theory*, Seventh edition, McGraw-Hill Inc., New York.